



CO, H₂O, H₂O⁺ line and dust emission in a z = 3.63 strongly lensed starburst merger at sub-kiloparsec scales



Chentao Yang^{1,†}, Raphael Gavazzi², Alexandre Beelen³, Pierre Cox², Alain Omont², Matthew Lehnert² et al. 2019, *A&A*, 624, A138

1. European Southern Observatory, Chile; 2. Institut d'Astrophysique de Paris, France; 3. IAS-Orsay, France; ([†]ESO Fellow).

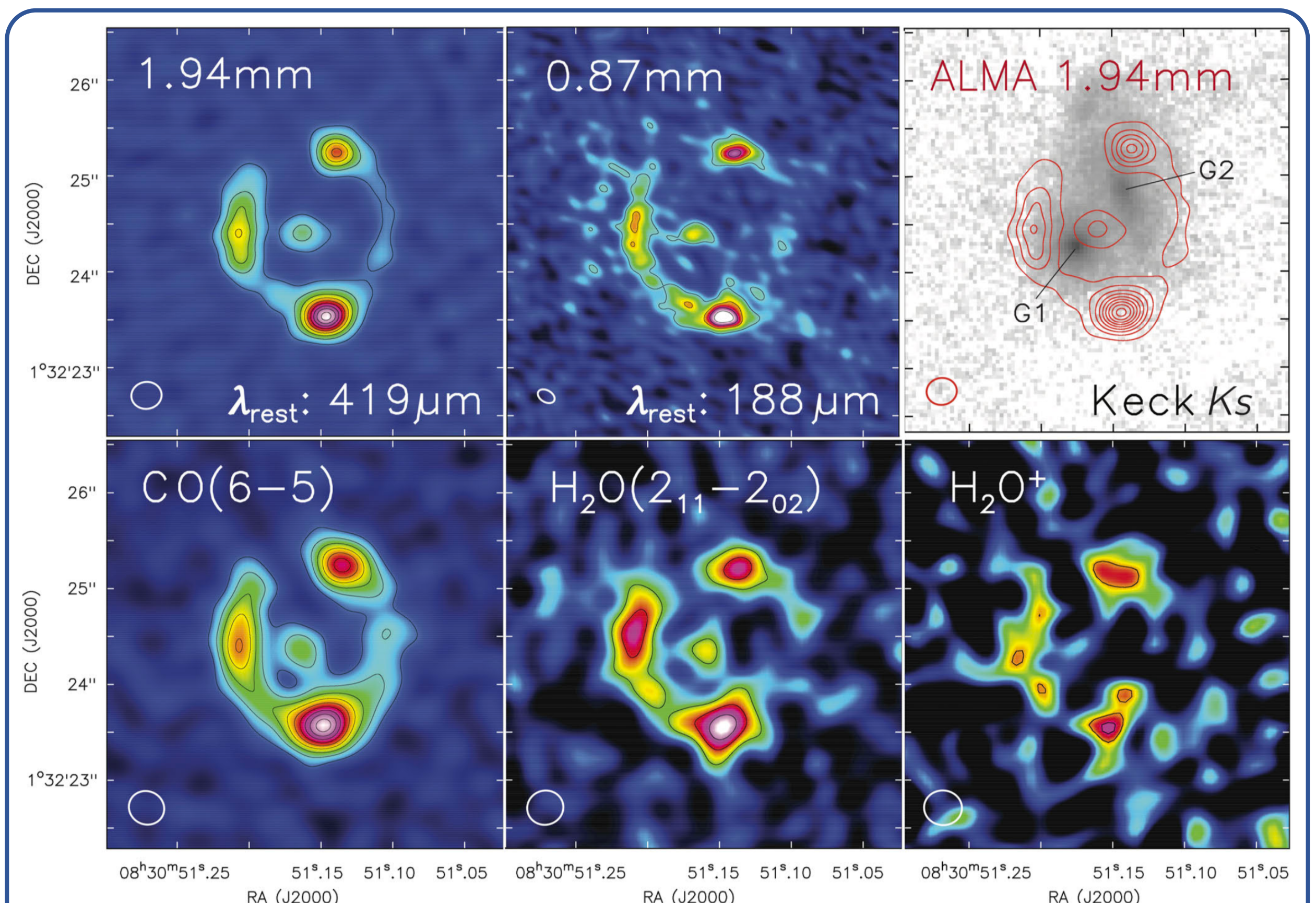


Fig. 1: 0.2"-0.4" arcsec resolution images of G09v1.97. The red contours show the dust continuum from G09v1.97 overlaid on the KECK images of the two deflectors, G1 and G2 at redshift 0.626 and 1.002, respectively.

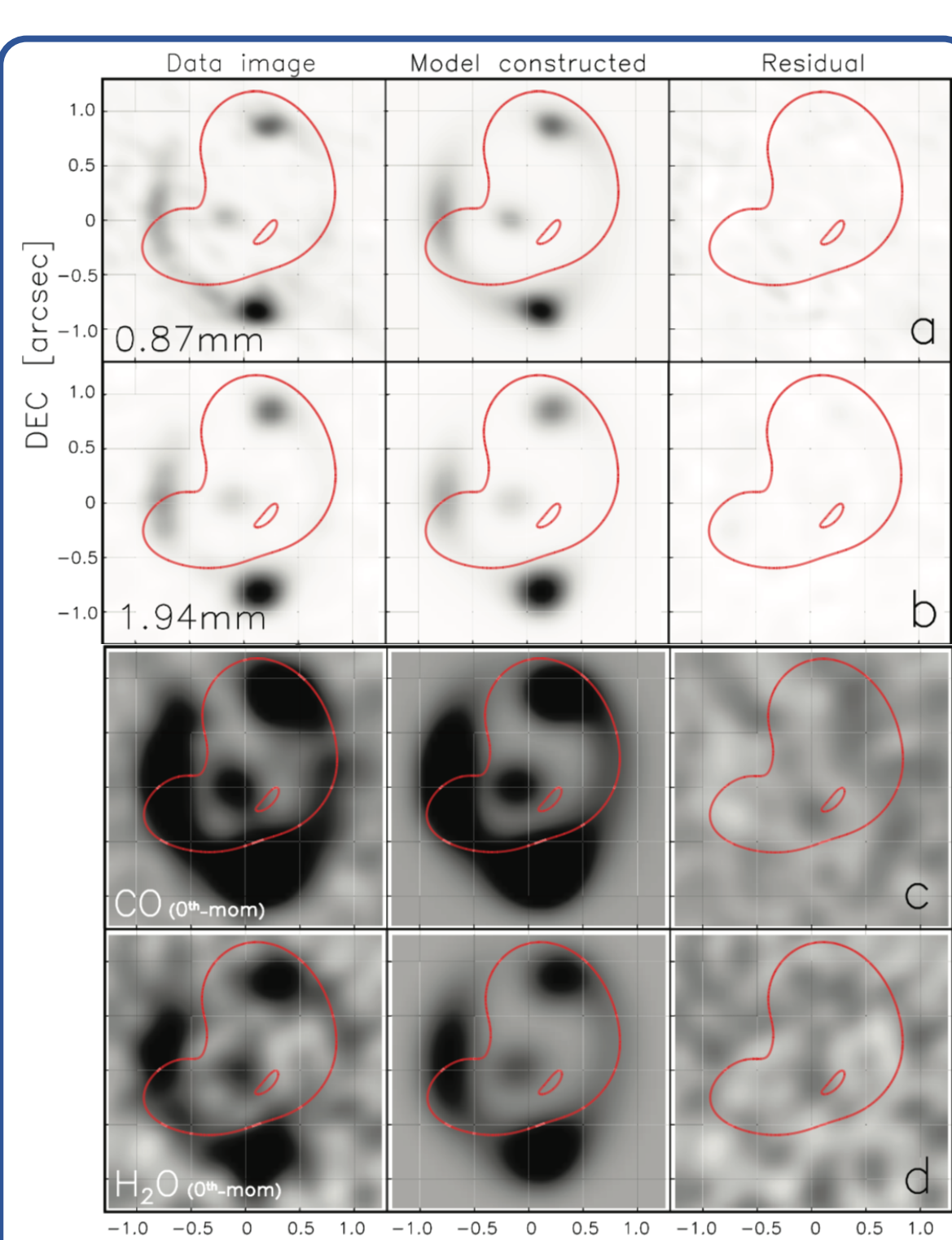


Fig. 3: Parametric lens model with an MCMC approach. The image plane data can be well reconstructed by the models.

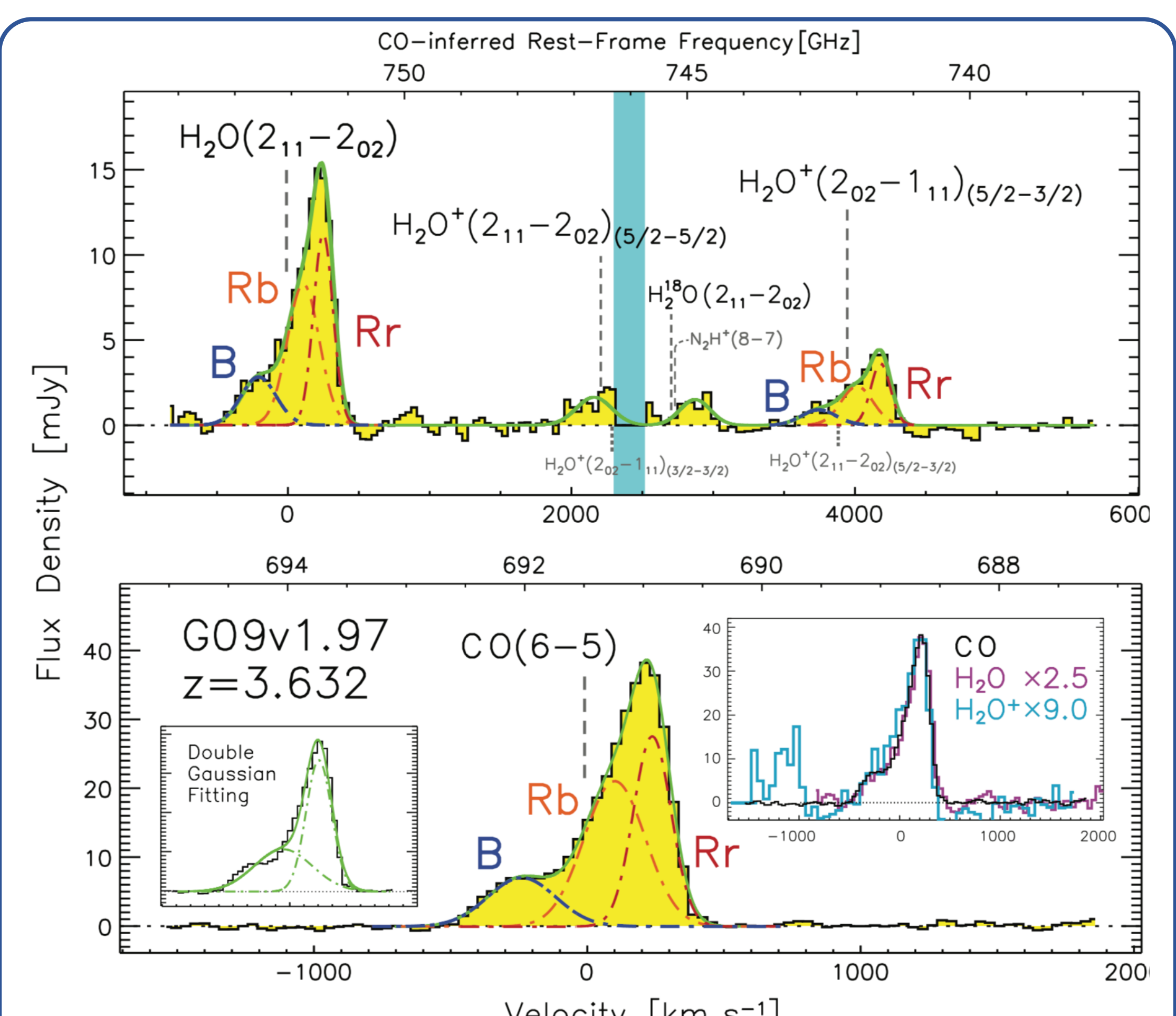
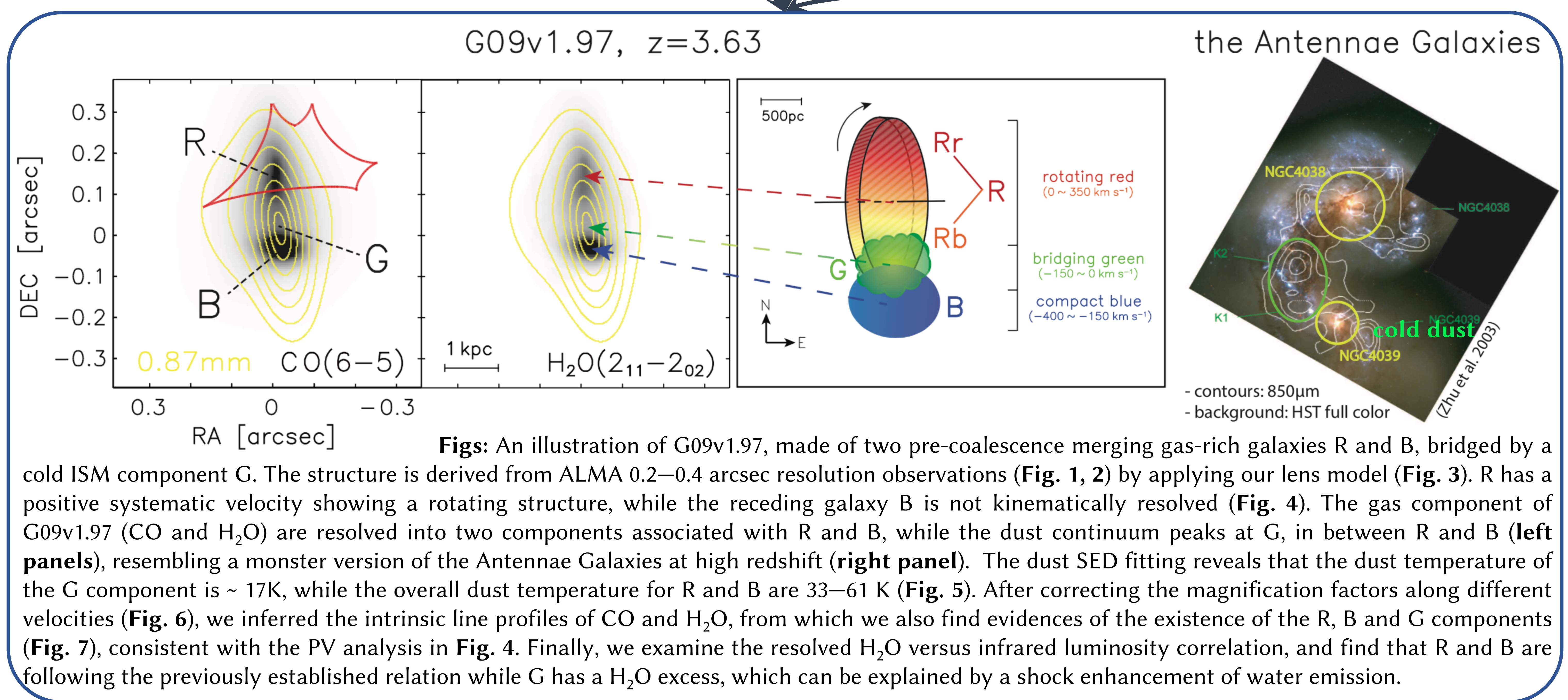


Fig. 2: Image-plane spatially integrated spectra of CO, H₂O and H₂O⁺ and H₂¹⁸O of G09v1.97. Multiple Gaussian components are needed, which reveal the physical components of G09v1.97.



Figs: An illustration of G09v1.97, made of two pre-coalescence merging gas-rich galaxies R and B, bridged by a cold ISM component G. The structure is derived from ALMA 0.2–0.4 arcsec resolution observations (Fig. 1, 2) by applying our lens model (Fig. 3). R has a positive systematic velocity showing a rotating structure, while the receding galaxy B is not kinematically resolved (Fig. 4). The gas component of G09v1.97 (CO and H₂O) are resolved into two components associated with R and B, while the dust continuum peaks at G, in between R and B (left panels), resembling a monster version of the Antennae Galaxies at high redshift (right panel). The dust SED fitting reveals that the dust temperature of the G component is ~ 17K, while the overall dust temperature for R and B are 33–61 K (Fig. 5). After correcting the magnification factors along different velocities (Fig. 6), we inferred the intrinsic line profiles of CO and H₂O, from which we also find evidences of the existence of the R, B and G components (Fig. 7), consistent with the PV analysis in Fig. 4. Finally, we examine the resolved H₂O versus infrared luminosity correlation, and find that R and B are following the previously established relation while G has a H₂O excess, which can be explained by a shock enhancement of water emission.

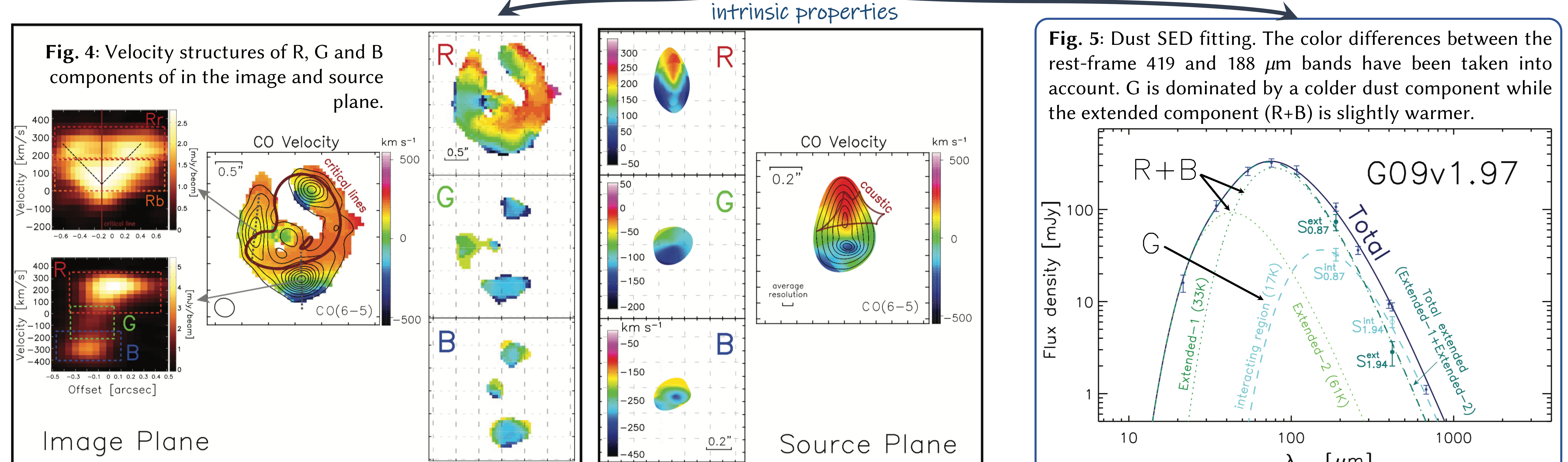


Fig. 5: Dust SED fitting. The color differences between the rest-frame 419 and 188 μm bands have been taken into account. G is dominated by a colder dust component while the extended component (R+B) is slightly warmer.

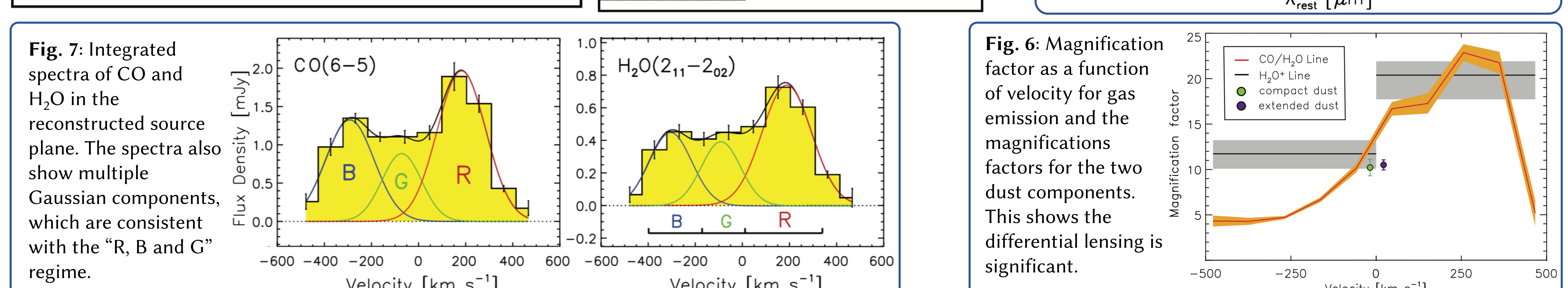


Fig. 7: Integrated spectra of CO and H₂O in the reconstructed source plane. The spectra also show multiple Gaussian components, which are consistent with the “R, B and G” regime.

Fig. 6: Magnification factor as a function of velocity for gas emission and the magnifications factors for the two dust components. This shows the differential lensing is significant.